

## TARGETING LOW-ENERGY TRANSFERS TO LOW LUNAR ORBIT

Jeffrey S. Parker\* and Rodney L. Anderson\*

A targeting scheme is presented to build trajectories from a specified Earth parking orbit to a specified low lunar orbit via a low-energy transfer and up to two maneuvers. The total transfer  $\Delta V$  is characterized as a function of the Earth parking orbit inclination and the departure date for transfers to each given low lunar orbit. The transfer  $\Delta V$  cost is characterized for transfers constructed to low lunar polar orbits with any longitude of ascending node and for transfers that arrive at the Moon at any given time during a month.

### INTRODUCTION

Modern trajectory design techniques have enabled the construction of new classes of low-energy trajectories that spacecraft may take to transfer between the Earth and the Moon. The Japanese Hiten mission is recognized as the first spacecraft to traverse a low-energy transfer from an orbit about the Earth to an orbit about the Moon.<sup>1,2</sup> The two ARTEMIS spacecraft recently navigated two very different low-energy transfers from their orbits about the Earth to lunar libration orbits near the Moon.<sup>3,4</sup> Both Hiten and ARTEMIS were extended missions that were enabled by their fuel-efficient low-energy transfers. The two GRAIL spacecraft are the first vehicles expecting to launch onto low-energy transfers as part of their primary mission, illustrated in Figure 1; they are also the first vehicles to transfer directly to low lunar orbits via low-energy transfers.<sup>5-7</sup> The success of Hiten, ARTEMIS, and hopefully GRAIL, have provided impetus to explore the trade space of low-energy lunar transfers in the expectation that such trajectories will continue to enable future missions.

Low-energy transfers between the Earth and the Moon are useful for a number of compelling reasons. First, a spacecraft following a practical low-energy transfer requires less fuel to achieve the same orbit than it would when following a conventional, 3–6 day direct transfer. The lunar orbit insertion maneuver is at least 100 m/s smaller when the spacecraft's destination is a 100 km circular orbit about the Moon.<sup>8</sup> The fuel savings are much more significant for spacecraft traveling to lunar libration orbits and other high three-body orbits, where spacecraft may save upwards of 500 m/s of the required  $\Delta V$  of a conventional transfer.<sup>9-12</sup> Low-energy transfers typically require 2–3 months more transfer duration than direct transfers. While this may be a disadvantage for missions with human passengers, it is a characteristic that carries several advantages for robotic missions. A spacecraft traversing a low-energy transfer may typically wait a week before performing a maneuver,<sup>6</sup> giving the spacecraft ample time to be checked out and prepare for its cruise operations. This also provides the spacecraft navigators ample time to achieve a stable solution of the spacecraft's orbit without requiring more than a handful of tracking stations. In addition, with several months of

---

\*Member of Technical Staff, Jet Propulsion Laboratory, California Institute of Technology, M/S 301-121, 4800 Oak Grove Dr., Pasadena, CA 91109

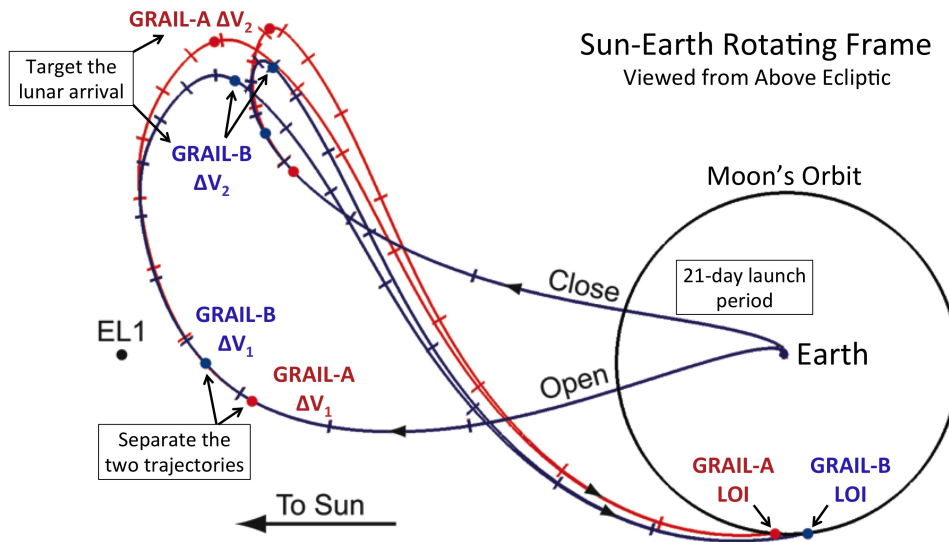


**Figure 1.** An illustration of GRAIL’s mission design, including a 21-day launch period and two deterministic maneuvers for both GRAIL-A and GRAIL-B, designed to separate their lunar orbit insertion times by 25 hours. Graphic courtesy of Roncoli and Fujii.<sup>5</sup>

transfer time a mission may be designed that places multiple spacecraft into different orbits at the Moon using a single launch vehicle without requiring a large amount of fuel. The GRAIL mission is one practical example: GRAIL’s two spacecraft are launched aboard the same Delta II rocket and each performs two deterministic maneuvers during their trans-lunar cruises to separate their lunar arrival times by 25 hours.<sup>5,6</sup> This separation is a benefit to the spacecraft operations team. Finally, another compelling reason to use a low-energy transfer for a robotic mission to the Moon is that one can construct a realistic 21-day launch period using minimal fuel, as will be demonstrated in this paper. GRAIL’s mission involves at least 21 launch opportunities, such that any launch date sends the two spacecraft on two transfers that arrive at the Moon on the same two dates, again separated by 25 hours. Conventional lunar transfers can achieve the same result, though they typically require numerous Earth phasing orbits and/or lunar flybys that add complexity and radiation exposure to the mission.

Numerous researchers have explored the trade space of low-energy lunar transfers since the 1960s using a variety of different techniques. In 1968, Charles Conley was among the first people to demonstrate that a trajectory may be designed to place a spacecraft in an orbit temporarily captured by the Moon without requiring an orbit insertion maneuver.<sup>13</sup> His technique takes advantage of dynamical systems tools found in the planar circular restricted three-body problem. Later, in 1990, Belbruno and Miller developed a targeting technique to design a low-energy trajectory for the Hiten mission.<sup>1</sup> Ivashkin is among many other people to employ similarly useful targeting techniques to generate low-energy lunar transfers.<sup>14,15</sup> Since 2000, several authors have continued to explore the dynamical systems methodology that Conley explored to generate low-energy transfers.<sup>16</sup> No practical methods have ever been found to analytically generate a low-energy transfer; hence, all progress to date has involved some sort of numerical or iterative technique to build the transfers.

Recent work has begun to systematically survey the trade space of low-energy lunar transfers by building entirely ballistic transfers between the Earth and (1) lunar libration orbits,<sup>9-11</sup> (2) low

lunar orbits,<sup>8</sup> and (3) the lunar surface.<sup>17,18</sup> These surveys have produced many thousands of lunar transfers that require no deterministic maneuvers whatsoever during their trans-lunar cruise. However, these transfers depart the Earth from particular Earth orbits and arrive at the Moon in a specified way, neither of which may be desirable for a practical mission. A previous paper studied the problem of transferring from a specified 28.5° circular low Earth orbit (LEO) to a particular lunar libration orbit using 1–3 maneuvers.<sup>12</sup> That paper presented a robust algorithm to generate a practical transfer, but it focused on only a handful of transfers to lunar libration orbits; it did not establish any statistically significant trends to predict the cost of an arbitrary transfer.

The work presented here is an extension of the research presented in these previous papers. The targeting algorithm presented in this paper is a modification of the algorithm used in Reference 12, applied to the problem of constructing a useful transfer from a specified LEO parking orbit to one of the transfers presented in Reference 8, each of which arrived at the Moon in 100-km circular polar lunar orbits. Details of these procedures are described in the next sections.

The purpose of this paper is to characterize the  $\Delta V$  cost needed to connect a particular low-energy lunar transfer, i.e., one with a desirable lunar approach, with a specified LEO parking orbit at the Earth departure point. The work presented here characterizes the  $\Delta V$  cost needed to generate a realistic, 21-day launch period for a collection of 288 low-energy transfers from 28.5° LEO parking orbits to polar lunar orbits. This effectively identifies the  $\Delta V$  cost needed to implement a low-energy transfer, taking it from a theoretical study to a practical trajectory.

## METHODOLOGY

Each low-energy transfer constructed in this paper departs the Earth, coasts to the Moon, and inserts directly into a circular 100 km polar orbit about the Moon. This lunar orbit is akin to the mapping orbits of several spacecraft, including Lunar Prospector,<sup>19</sup> Kaguya/SELENE,<sup>20</sup> Chang’e 1,<sup>21</sup> Chandrayaan-1,<sup>22</sup> the Lunar Reconnaissance Orbiter,<sup>23</sup> and GRAIL.<sup>5</sup> Figure 2 illustrates an example 84-day low-energy transfer. The following sections provide more information about each phase of this example low-energy transfer and how it compares with other lunar transfers.

**Earth Parking Orbit** The low-energy lunar transfers designed here depart the Earth from 185-km circular parking orbits. Unless otherwise noted, the parking orbits have inclinations of 28.5° in the EME2000 coordinate frame, i.e., an inertial frame aligned with the Earth’s mean equator on January 1, 2000 at 12:00:00 UTC. This inclination corresponds to an easterly launch from Cape Canaveral, Florida. For the purposes of this paper, the actual launch time and its bearing on the orientation of the surface of the Earth is not considered; hence, Cape Canaveral is not constrained to be beneath the parking orbit. Adjusting the launch time by as many as 12 hours typically only has a slight impact on the trajectory and its corresponding launch period.

**Trans-Lunar Injection** The Trans-Lunar Injection (TLI) is modeled as an impulsive  $\Delta V$  tangent to the parking orbit. This maneuver is typically performed by the launch vehicle. The launch vehicle’s target  $C_3$  value is typically in the range of -0.7 to -0.4 km<sup>2</sup>/s<sup>2</sup>, where  $C_3$  is a parameter equal to twice the target specific energy. Since this target is negative, the resulting orbit is still captured by the Earth. If the trajectory is designed to implement a lunar gravity assist on the way out to the long cruise, then the launch target may be reduced to a  $C_3$  of approximately -2 km<sup>2</sup>/s<sup>2</sup>.

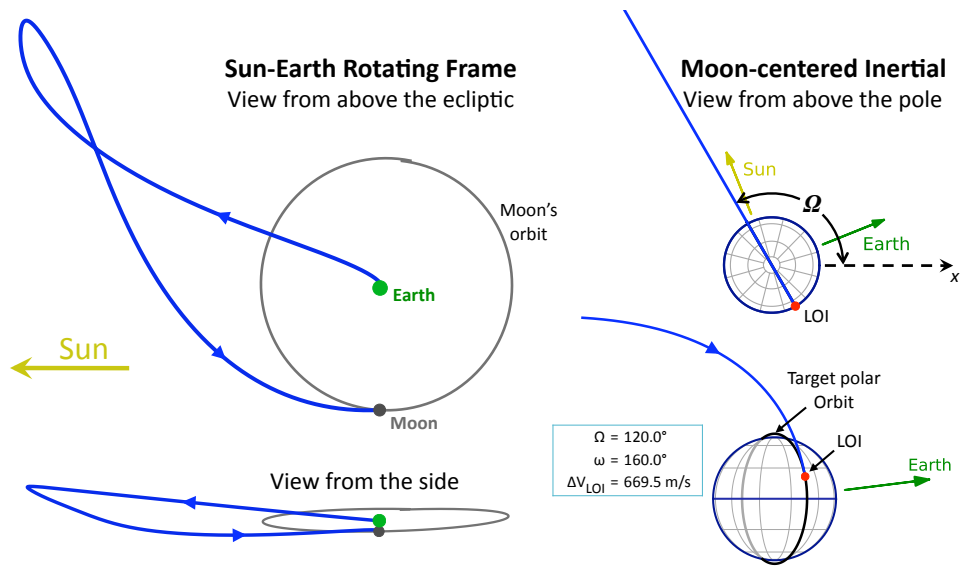


**Figure 2. An example 84-day low-energy transfer between the Earth and a 100 km circular polar lunar orbit.**

Launch vehicles typically target the right ascension and declination of the outbound asymptote for interplanetary missions to other planets. Since a low-energy lunar transfer is still captured by the Earth there is no outbound asymptote; hence, the GRAIL targets include the right ascension and declination of the instantaneous apogee vector at the target interface time.<sup>5</sup>

**Trans-Lunar Cruise** A spacecraft's trans-lunar cruise on its low-energy lunar transfer takes it beyond the orbit of the Moon and typically in a direction toward either the second or fourth quadrant in the Sun-Earth synodic coordinate system.<sup>24</sup> The spacecraft typically ventures 1–2 million kilometers away from the Earth, where the Sun's gravity becomes very influential. As the spacecraft traverses its apogee the Sun's gravity constantly pulls on it, raising the spacecraft's perigee altitude. By the time the spacecraft begins to return to the Earth its perigee has risen high enough that it encounters the Moon. Further, the trajectory is designed to place the spacecraft on a lunar encounter trajectory. The GRAIL mission design involves two deterministic maneuvers and three statistical maneuvers for each spacecraft to navigate its trans-lunar cruise.<sup>6</sup> The transfers in this paper may include up to two deterministic maneuvers performed during the trans-lunar cruise. These maneuvers are constrained to be further than four days from any other maneuver.

**Lunar Orbit Insertion** The Lunar Orbit Insertion (LOI) is modeled as an impulsive  $\Delta V$  that inserts the spacecraft directly into the target 100 km circular lunar orbit. A typical lunar mission inserts into a large temporary *capture* orbit before descending into the final target orbit. This sort of mission design reduces gravity losses and protects the spacecraft in the event of an overburn. The LOI is not required to be tangent to the target orbit in this study if a small plane change would reduce the total transfer  $\Delta V$  of the mission.

**Target Lunar Orbit** The target lunar orbits in this paper are 100-km circular polar orbits, defined in a coordinate frame that is centered at the Moon and aligned with the lunar spin axis. The  $z$ -axis extends from the center of the Moon toward its northern spin-axis pole at the time of the LOI; the  $x$ -axis extends toward the point where the Moon’s equatorial plane ascends through the Earth’s J2000 equatorial plane; the  $y$ -axis completes the right-handed coordinate frame.<sup>25</sup> The  $x$ -axis points within  $3.77^\circ$  of Earth’s vernal equinox at any given time. It may be the case that a mission’s design requires an elliptical lunar orbit such that its orientation about the Moon is a mission requirement; for instance, a mission may be designed to place a communication satellite into an elliptical orbit with its apoapse over the lunar south pole. In this paper, the LOI is performed at the orbit’s periapse point and the orbit’s orientation, i.e., its argument of periapsis and longitude of ascending node, is specified and fixed. In this way, one may target a particular lunar orbit and study the  $\Delta V$  costs required to insert into that orbit.

## Models

All trajectories generated in this study are propagated using the DIVA propagator, which implements a variable order Adams method.<sup>26</sup> The state integration tolerance has been set to  $1 \times 10^{-10}$ .

The gravity model includes the Sun, Earth, and Moon at all times, modeled as point-masses with  $GM$  values of approximately  $1.327124 \times 10^{11} \text{ km}^3/\text{s}^2$ ,  $3.986004 \times 10^5 \text{ km}^3/\text{s}^2$ , and  $4.902800 \times 10^3 \text{ km}^3/\text{s}^2$ , respectively. The positions of each body are estimated using JPL’s DE421 Planetary Ephemerides.<sup>27</sup> The mean radius of the Earth and Moon are assumed to be 6378.1363 km and 1737.4 km, respectively.

The optimization package SNOPT (Sparse Nonlinear OPTimizer)<sup>28,29</sup> is used in this research to adjust the values of parameters in a system in order to identify solutions that require minimal amounts of fuel. The algorithm is highly effective at identifying local minima in the state space of systems such as those encountered here, where the state space involves smooth nonlinear objective functions. The algorithm does not necessarily converge on the global minimum; hence it is common that the routine is executed with several sets of initial conditions to improve the probability that it encounters the optimal solution.

## Designing each Transfer

Each lunar mission is constructed here using a straightforward procedure that is described as follows.

**Step 1.** First, a target lunar orbit is selected and a reference low-energy lunar transfer is constructed. The transfers used here have been taken from the surveys presented in Reference 8.

Each target low lunar orbit is constructed here by setting its semi-major axis to 1837.4 km, its eccentricity to zero, and its inclination to  $90^\circ$ , as described previously. This defines a circular, polar orbit with an altitude of approximately 100 km. Its longitude of ascending node,  $\Omega$ , and argument of periapse,  $\omega$ , are selected from the surveys and can take on a wide variety of combinations.

An impulsive, tangential lunar orbit insertion is applied at the orbit’s periapse point on a specified date. The LOI  $\Delta V$  magnitude is taken from the surveys. It is set to generate a trajectory that originates at the Earth via a simple low-energy transfer: one that contains no close lunar encounters or Earth phasing orbits. The  $\Delta V$  value is at least 640 m/s and is the

**Table 1. A summary of the performance parameters of several example simple low-energy lunar transfers. None of these transfers includes any Earth phasing orbits or lunar flybys.**

| Traj # | $\Omega$ (deg) | $\omega$ (deg) | $\Delta V_{\text{LOI}}$ (m/s) | Duration (days) | LEO Inclination (deg) |          | $C_3$ ( $\text{km}^2/\text{s}^2$ ) |
|--------|----------------|----------------|-------------------------------|-----------------|-----------------------|----------|------------------------------------|
|        |                |                |                               |                 | Equatorial            | Ecliptic |                                    |
| 1      | 120.0          | 169.2          | 669.3                         | 83.483          | 29.441                | 6.129    | -0.723                             |
| 2      | 120.0          | 103.8          | 692.1                         | 85.287          | 25.688                | 34.778   | -0.723                             |
| 3      | 120.0          | 70.2           | 743.9                         | 93.598          | 57.654                | 74.955   | -0.667                             |
| 4      | 120.0          | 225.3          | 716.0                         | 93.621          | 134.322               | 112.840  | -0.657                             |
| 5      | 120.0          | 99.9           | 697.5                         | 110.060         | 83.127                | 61.624   | -0.697                             |
| 6      | 120.0          | 186.9          | 673.2                         | 122.715         | 23.941                | 3.088    | -0.712                             |

least  $\Delta V$  needed to construct a transfer that requires fewer than 160 days to reach an altitude of 1000 km or less above the Earth when propagated backward in time. Table 1 summarizes several example transfers that target low lunar orbits that each have an  $\Omega$  of  $120^\circ$ , taken from a survey found in Reference 8.

Each reference trajectory generated in this study has no maneuvers and does not target any particular Earth orbit when propagated backward in time.

**Step 2.** Second, the mission’s LEO parking orbit and Trans-Lunar Injection time are specified. The LEO parking orbits used in this paper are all 185-km circular orbits with inclinations of  $28.5^\circ$ , as previously described. The orbit’s node,  $\Omega_{\text{LEO}}$ , and the location of the TLI maneuver about the orbit,  $\nu_{\text{LEO}}$ , are permitted to vary; the TLI is performed tangent to the orbit.

**Step 3.** The low-energy transfer is adjusted to have a perigee that coincides with the time of the TLI. This is performed by using SNOPT to determine the smallest change in the LOI  $\vec{\Delta V}$  that results in a new low-energy transfer that originates at the Earth on the date of the TLI, or at least one that has a perigee on that date even if the perigee altitude is higher than 1000 km.

**Step 4.** The radius of the low-energy transfer with respect to the Earth at a time 20 days after the TLI is noted. The TLI  $\Delta V$  magnitude,  $\Delta V_{\text{TLI}}$ , is set to a value that takes the Earth-departure trajectory out to that distance at that time, using some initial guess for the orientation of the parking orbit at that time. The spacecraft is beyond the orbit of the Moon by that time, assuming no Earth phasing orbits, and not yet at its apogee.

**Step 5.** The optimization algorithm SNOPT is used to identify the values of  $\Omega_{\text{LEO}}$  and  $\nu_{\text{LEO}}$  that minimize the difference in position between the Earth-departure and the target low-energy transfer at a time 20 days after TLI. After convergence, the algorithm is repeated, this time permitting  $\Delta V_{\text{TLI}}$  to vary as well. It is typically the case that the Earth-departure trajectory will intersect the target low-energy transfer at that time when all three variables are permitted to vary, though it is not necessary.

**Step 6.** Two deterministic maneuvers are added to the trajectory: TCM1 at a time 21 days after TLI, and TCM2 at a time halfway between TCM1 and LOI. It is intentional that the first maneuver be placed near 20 days but not at a value of 20 days in order to improve the performance of the optimization algorithm in the next step.<sup>12</sup>

**Step 7.** The SNOPT algorithm is implemented again to converge on an end-to-end trajectory between the specified LEO parking orbit and the specified low lunar orbit, minimizing the total

transfer  $\Delta V$ . This optimization includes eight variables: the three Earth-departure parameters  $\Omega_{\text{LEO}}$ ,  $\nu_{\text{LEO}}$ , and  $\Delta V_{\text{TLI}}$ , the dates of the two trans-lunar maneuvers  $t_{\text{TCM1}}$  and  $t_{\text{TCM2}}$ , and the three components of the LOI  $\Delta V$ , namely,  $\Delta V_{\text{LOI}}^x$ ,  $\Delta V_{\text{LOI}}^y$ , and  $\Delta V_{\text{LOI}}^z$ . When the eight parameters are adjusted, an Earth-departure trajectory is generated out to the time of TCM1, a lunar-arrival trajectory is generated backward in time from LOI to the time of TCM2, and a bridge trajectory is generated connecting TCM1 and TCM2 using a single-shooting differential corrector.<sup>12,30</sup> The optimization algorithm is set to minimize the sum of the maneuvers that are typically required by the spacecraft, namely, the sum of  $\Delta V_{\text{TCM1}}$ ,  $\Delta V_{\text{TCM2}}$ , and  $\Delta V_{\text{LOI}}$ , but not the TLI  $\Delta V$ . The dates of the TLI and LOI are fixed, and the dates of TCM1 and TCM2 are constrained to be at least four days from any other maneuver to facilitate relaxed spaceflight operations.

When the optimizer has converged, the performance of the trajectory compared with the reference low-energy transfer is recorded. It is often the case that the differential corrector will converge on a local minimum and not the global minimum; hence, this process is repeated with adjustments in the eight parameters to identify the lowest local minimum possible. This will be discussed more later.

To summarize, this procedure constructs a practical, two-burn, low-energy lunar transfer between a specified Earth departure and a specified lunar arrival. The altitude, eccentricity, and inclination of the Earth parking orbit are specified and fixed, as is the date of the Trans-Lunar Injection maneuver. The target lunar orbit, the LOI position, and the LOI date are all specified and fixed. The TLI maneuver is constrained to be tangential to the parking orbit, though the orientation of the parking orbit may vary; the LOI maneuver is not constrained to be tangential. Finally, the dates of two trans-lunar maneuvers and their  $\Delta V$  values are permitted to vary.

## AN EXAMPLE LUNAR MISSION

This section demonstrates the process of generating a practical low-energy lunar transfer. A reference lunar transfer has been selected from the surveys presented in Reference 8, including a target lunar orbit and LOI date. Several key parameters of this mission are summarized in Table 2. The resulting low-energy lunar transfer, illustrated in Figure 3, has a transfer duration of 101.6 days, naturally originating at the Earth on April 1, 2010 at 05:27 UTC. The reference Trans-Lunar Injection has a TLI  $\Delta V$  magnitude of approximately 3195.635 m/s, corresponding to a  $C_3$  of  $-0.713003 \text{ km}^2/\text{s}^2$ , and it departs from a circular 185-km LEO parking orbit with an inclination of approximately  $38.305^\circ$ .

**Table 2. A summary of the parameters used to generate the reference low-energy lunar transfer used in the example lunar mission.**

| Parameter                   | Value                      |
|-----------------------------|----------------------------|
| Target Lunar Orbit $\Omega$ | 257.430 deg                |
| Target Lunar Orbit $\omega$ | 48.268 deg                 |
| Date of LOI                 | July 11, 2010 at 19:41 UTC |
| $\Delta V_{\text{LOI}}$     | 649.00 m/s                 |

To illustrate the entire process of building a practical lunar transfer, we will set the Earth departure to take place from a parking orbit at an inclination of  $28.5^\circ$  one day later than the reference

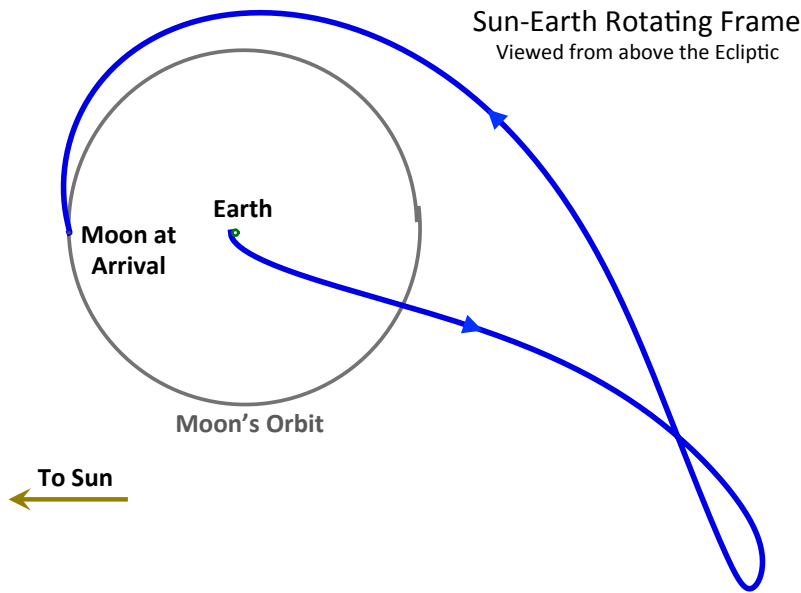


**Figure 3.** An illustration of the example reference low-energy lunar transfer, shown in the Sun-Earth rotating frame from above the ecliptic, where the Sun is fixed to the left.

trajectory’s departure on April 2, 2010 at 05:27 UTC. A launch vehicle may certainly target a departure at an inclination of  $38.3^\circ$ , but the performance loss is typically significant. The procedure outlined here results in a small increase of onboard propellant to make the adjustment.

Table 3 tracks the values of the eight control variables and the transfer  $\Delta V$  cost as the lunar mission is constructed, following the steps outlined above. The reference trajectory is summarized in Step #1: the only control variables set are the components of the LOI  $\Delta V$ . Step #2 does not change any control variables and is hence not shown. Step #3 illustrates the small change in the components of the LOI  $\Delta V$  vector that are required to shift the timing of the trajectory’s perigee to coincide with the TLI maneuver. The adjustment amounts to a difference of only 3.3 cm/s in the LOI  $\Delta V$  magnitude. Although this new trajectory’s perigee occurs on April 2, 2010 at 5:27 UTC, the

**Table 3.** The history of the example lunar transfer’s control variables as the mission is constructed, where  $\Delta t_{TCM1}$  is the duration of time between TLI and TCM1 and  $\Delta t_{TCM2}$  is the duration of time between TCM1 and TCM2.

| Step # | TLI Parameters |           |                | TCM1            |                | TCM2            |                | LOI   |         |  | Total Transfer $\Delta V$ , m/s |
|--------|----------------|-----------|----------------|-----------------|----------------|-----------------|----------------|---|---------|--|---------------------------------|
|        | $\Omega$ deg   | $\nu$ deg | $\Delta V$ m/s | $\Delta t$ days | $\Delta V$ m/s | $\Delta t$ days | $\Delta V$ m/s | $\Delta V_x$ , $\Delta V_y$ , and $\Delta V_z$ m/s, EME2000 |         |  |                                 |
| 1      | -              | -         | -              | -               | -              | -               | -              | -87.728, -271.090, -583.108                                 | -       |  |                                 |
| 3      | -              | -         | -              | -               | -              | -               | -              | -87.732, -271.103, -583.138                                 | -       |  |                                 |
| 4      | 0.00           | 0.00      | 3197.44        | -               | -              | -               | -              | -87.732, -271.103, -583.138                                 | -       |  |                                 |
| 5      | -25.00         | 27.18     | 3196.77        | -               | -              | -               | -              | -87.732, -271.103, -583.138                                 | -       |  |                                 |
| 6      | -25.00         | 27.18     | 3196.77        | 21.00           | 26.10          | 34.84           | 6.37           | -87.732, -271.103, -583.138                                 | 681.500 |  |                                 |
| 7      | -25.08         | 27.32     | 3196.79        | 20.63           | 24.09          | 34.86           | 0.00           | -87.736, -271.118, -583.167                                 | 673.155 |  |                                 |

perigee altitude is no longer 185 km but has risen to about 5200 km. Steps #4 – #6 construct initial guesses for the departure parameters and place two deterministic maneuvers en route to construct a complete end-to-end trajectory. Finally, Step #7 includes the full optimization, where all eight parameters are permitted to vary and the transfer  $\Delta V$  is minimized.

During Step #4, initial guesses for  $\Omega_{\text{TLI}}$  and  $\nu_{\text{TLI}}$  are needed. In this example they are both set to  $0^\circ$ , however, it has been observed that the entire procedure may converge to different local minima using different combinations of initial guesses for these parameters. There are often two local minima that correspond to the typical *short* and *long* coasts for the Earth departure. In addition, the process often converges on different local minima depending on the propagation duration of the initial Earth departure. In this research, we have opted to perform Steps #4 – #6 numerous times with different initial guesses and then send only the best one or two trajectories into Step #7. This process ensures that the majority of local minima are explored without spending too much time in Step #7, which is by far the most computationally demanding step. It is likely that additional small improvements may be made, but this procedure generates a reliable estimate of the minimum transfer  $\Delta V$  given a reference lunar transfer.

One can see in the final row of Table 3 that the optimizer has converged on a solution that drove the second deterministic  $\Delta V$  to zero. This is typical behavior for this algorithm when the trajectory is not required to change far from the reference, i.e., when the date of the TLI is within a few days of the reference trajectory and/or when the LEO parking orbit's inclination is within several degrees of the reference trajectory's perigee inclination.

Figure 4 illustrates the difference between the Earth departures of the reference trajectory and the final, targeted lunar transfer generated here. The inclination change and the shift in the TLI departure date are compensated by the  $\sim 24.1$  m/s of trans-lunar  $\Delta V$ . Figure 5 shows a comparison of the final transfer and the reference transfer, viewed from above the ecliptic in the Sun-Earth rotating frame. One can see that the geometry and the general features of the final transfer have not changed significantly during the procedure.

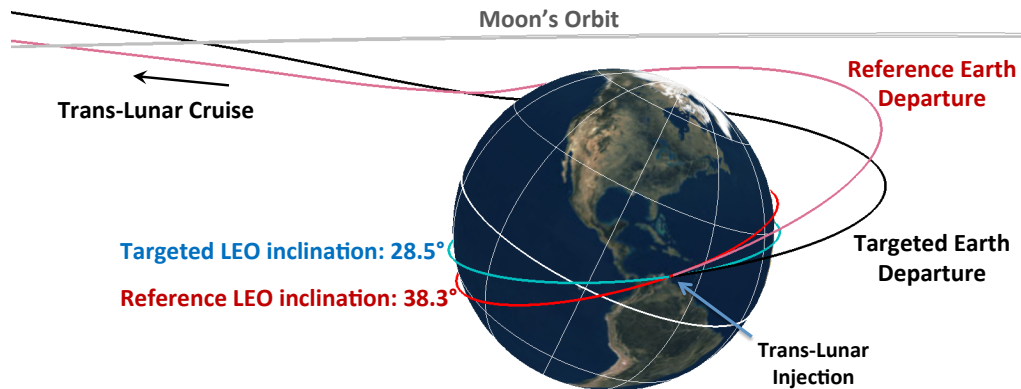


**Figure 4. The targeted Earth departure compared with the reference Earth departure.**

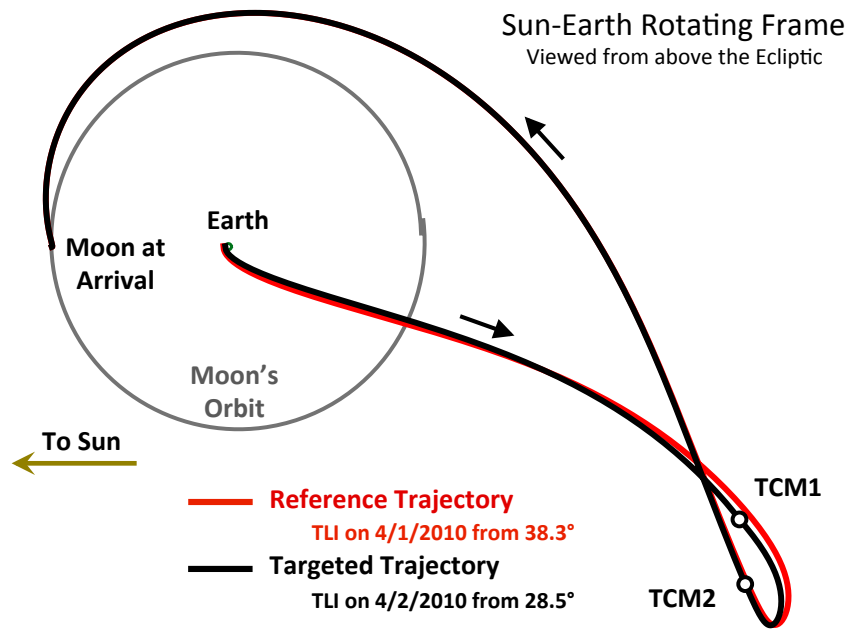


**Figure 5. The final targeted lunar transfer compared to the reference transfer, viewed in the Sun-Earth rotating frame from above the ecliptic.**

## BUILDING A LAUNCH PERIOD

The process described above may be repeated for each day in a wide range of dates to identify a practical launch period. The total transfer  $\Delta V$  typically rises as the TLI date is adjusted further from a reference trajectory's TLI date. In this research, we search 30 days on either side of the reference trajectory's TLI date and identify a practical 21-day launch period within those 61 days. The 21 days of opportunities do not have to be consecutive, though they are typically collected in either one or two segments. Since low-energy transfers travel beyond the orbit of the Moon, they may interact with the Moon as they pass by, even if they pass by at a great distance. The Moon may boost or reduce the spacecraft's energy as it passes by, depending on the geometry; typically there is a point in a launch period where the geometry switches.

Figure 6 illustrates the transfer  $\Delta V$  cost required to target the reference lunar transfer studied in the previous section as a function of TLI date. Each transfer has been generated using the procedure outlined previously, but with a different TLI date. The trajectories that launch 5–6 days prior to the reference transfer are significantly perturbed by the Moon, though not perturbed enough to break the launch period into two segments. One can see that the least expensive 21-day launch period requires a transfer  $\Delta V$  of approximately 706.2 m/s.

## REFERENCE TRANSFERS

A total of 288 reference transfers have been used to generate lunar missions with realistic, 21-day launch periods, each starting from a  $28.5^\circ$  LEO parking orbit. These reference trajectories have been randomly sampled from low- $\Delta V$ , simple, low-energy transfers presented in the surveys found in Reference 8. The trajectories target low lunar orbits with any longitude of ascending node and with any argument of periapsis, though the combination of those parameters must yield

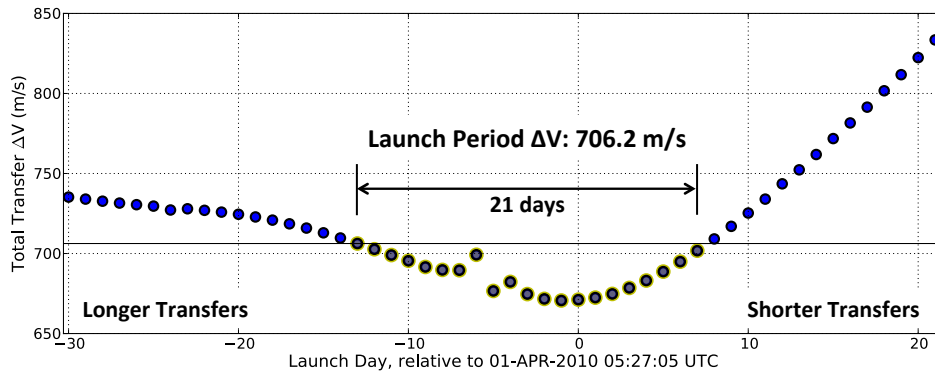


**Figure 6.** An example 21-day launch period, constructed using the reference lunar transfer presented in Figure 3.

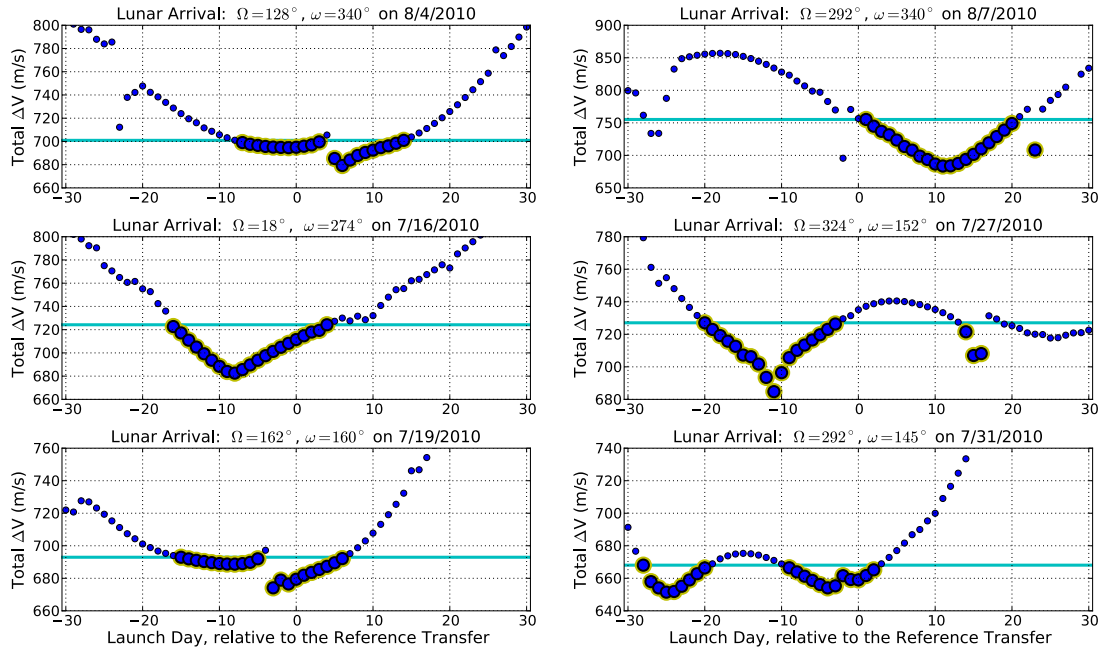
a satisfactory reference transfer. The transfers arrive at the Moon at any of 8 arrival times evenly distributed across a synodic month between July 11, 2010 at 19:41 UTC and August 6, 2010 at 20:37 UTC. The majority of the reference transfers sampled here implement lunar orbit insertion maneuvers with magnitudes between 640 m/s and 750 m/s, though reference transfers have been sampled with LOI  $\Delta V$  values as high as 1080 m/s. Finally, reference transfers have been sampled with transfer durations between 65 and 160 days. This collection of reference transfers makes no assumptions about what sort of mission a designer may be interested in, except that each transfer is simple, i.e., it includes no Earth phasing orbits nor lunar flybys, and each transfer targets a polar lunar orbit.

## RESULTS

In general, the algorithms described in this paper generate successful launch periods with similar characteristics. Figure 7 illustrates the total transfer  $\Delta V$  of several example launch periods that have been generated from these reference transfers. One notices that many of these launch periods include a single main convex  $\Delta V$  minimum, from which a 21-day launch period is easily identified. Other  $\Delta V$  curves include two or more local minima. The launch periods are designed to have at most two gaps, where each gap must be less than 14 days in extent. A particular lunar mission may have different requirements, which may improve the launch period's cost.

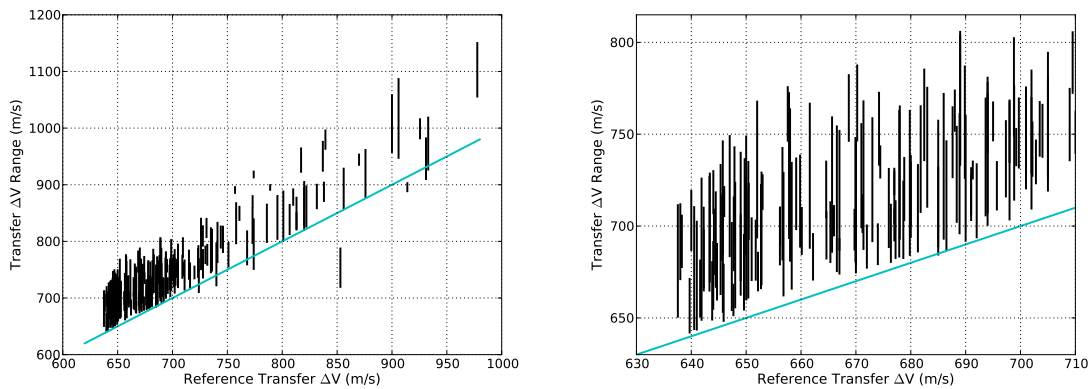
It has been found that most 21-day launch periods among the 288 missions studied include the reference launch date, though there are many examples that do not, including two of those shown in Figure 7. In some cases a practical launch period may have extended further than 30 days from the reference launch date and required less total  $\Delta V$ . There are often sudden jumps in the transfer  $\Delta V$  curves, which are caused by the Moon's perturbation as the spacecraft departs the Earth. Since each transfer in a particular launch period departs the Earth in approximately the same direction, the Moon passes near the transfer's outbound leg about once every synodic month. Some transfers do not experience any significant perturbations due to their out-of-plane motion.

Figure 8 illustrates the range of the transfer  $\Delta V$  values that are contained in each 21-day launch period as a function of their reference transfer  $\Delta V$ . As an example, the launch period illustrated in Figure 6 was generated using a reference transfer with a  $\Delta V$  of 649 m/s (the ordinate of the plots in Figure 8) and the resulting launch period included missions that had transfer  $\Delta V$  values



**Figure 7.** Several example curves that illustrate the post-TLI  $\Delta V$  cost of transferring from a  $28.5^\circ$  LEO parking orbit at different TLI dates to a given reference low-energy transfer, including a highlighted 21-day launch period in each case.

between 670.6 and 706.2 m/s. One can see that the majority of transfers studied here have reference transfer  $\Delta V$  values less than 750 m/s, though the transfers sampled include those with reference  $\Delta V$  values up to 1080 m/s. The launch period  $\Delta V$  range often starts above the mission's reference  $\Delta V$  since each mission starts from a  $28.5^\circ$  LEO parking orbit and the reference transfer typically



**Figure 8.** The range of transfer  $\Delta V$  values contained in each 21-day launch period as a function of the reference transfer  $\Delta V$ . The plot on the right shows an exploded view of the low- $\Delta V$  transfers.

departs from some other inclination. In a few cases, and one extreme case, the launch period  $\Delta V$  range starts below the reference  $\Delta V$ . This is often possible when the reference transfer has a natural Earth departure far from  $28.5^\circ$  and a change in the transfer duration reduces the total  $\Delta V$ . The plots in Figure 8 clearly illustrate that the  $\Delta V$  cost of establishing a 21-day launch period is highly dependent on the reference transfer's total  $\Delta V$ . The launch period  $\Delta V$  cost of these 288 example transfers requires approximately  $71.67 \pm 29.71$  m/s ( $1\sigma$ ) more deterministic  $\Delta V$  than the transfer's reference  $\Delta V$ .

The launch periods studied here include missions that depart the Earth on 21 different days and the launch period  $\Delta V$  cost is the  $\Delta V$  of the most expensive transfer in that set. The departure days do not need to be consecutive, as described earlier. In general, increasing the number of launch days included in a launch period increases the  $\Delta V$  cost of the mission. Figure 9 shows a plot of the change in the launch period  $\Delta V$  cost of the 288 missions studied here as one adds more days to each mission's launch period, relative to the case where each mission has only a single launch day. The line of best fit through these data indicate that on average it requires approximately 2.480 m/s per launch day to add days to a mission's launch period. There is a significant jump in the launch period  $\Delta V$  when one moves from a 1-day launch period to a 2-day launch period. This is due to the fact that the Moon's perturbations often produce a single launch day with remarkably low  $\Delta V$  requirements. The change in a launch period's required  $\Delta V$  would be more smooth if the effects of lunar perturbations on the Earth-departure leg were ignored.

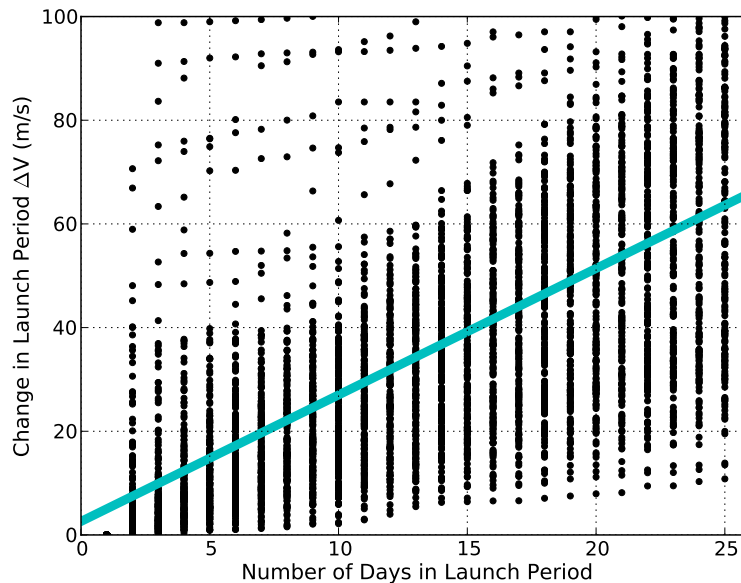


**Figure 9.** The change in the launch period  $\Delta V$  cost of the 288 missions studied here as a function of the number of days in the launch period. The linear trend has a slope of 2.480 m/s per launch day.

It has been noted when studying Figure 7 that a launch period does not necessarily include the reference launch date. However, it is expected that the transfer duration of a reference trajectory may be used to predict a mission's actual transfer duration. Figure 10 tracks the range of transfer durations within each 21-day launch period studied here as a function of the mission's reference transfer

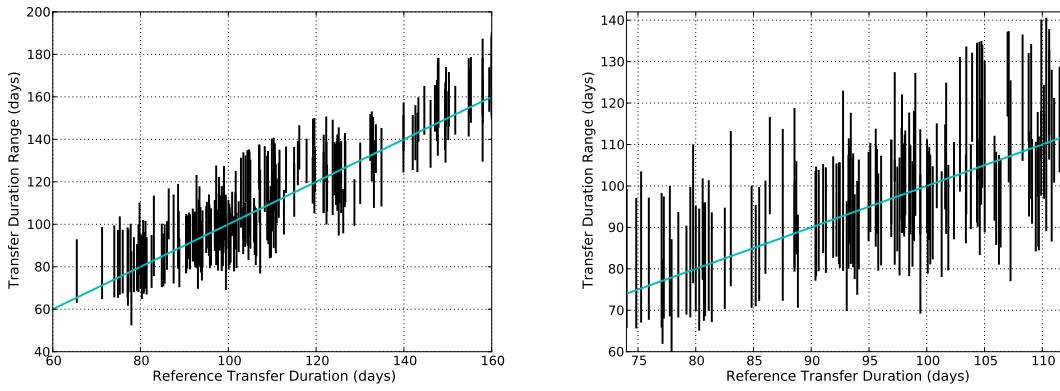


**Figure 10. The range of transfer durations contained in each 21-day launch period as a function of the reference transfer duration. The plot on the right shows an exploded view, focused on transfer durations between 75 and 115 days.**

duration. One can see that the range of transfer durations is indeed correlated with the reference transfer duration. Furthermore, it has been found that the maximum transfer duration of the 288 launch periods is approximately  $15.95 \pm 8.66$  days longer than the mission's reference duration, the minimum transfer duration is approximately  $10.91 \pm 7.75$  days shorter than the reference duration, and the total number of days between the first and final launch date of a given launch period may be estimated at approximately  $26.86 \pm 6.95$  days. Hence, one may predict that a mission's launch period will include 21 of about 27 days, centered on a date several days earlier than the reference launch date, if one constructs a 21-day launch period using the same rules invoked here.

Figure 11 tracks the range of  $\Delta V$  costs associated with each launch period as a function of the duration of the mission's reference transfer. One can see that there is a wide spread of transfer  $\Delta V$  across the range of durations. As the reference transfer duration drops below 90 days, the launch

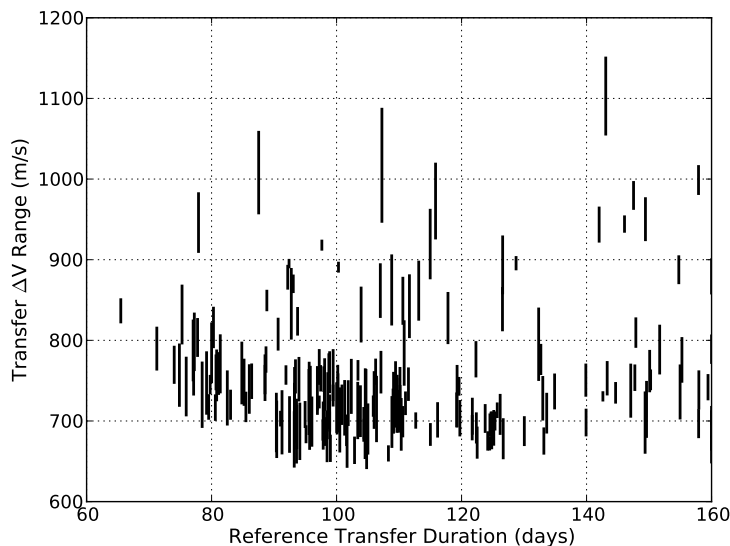


**Figure 11. The range of transfer  $\Delta V$  costs contained in each 21-day launch period as a function of the reference transfer's duration.**

period  $\Delta V$  cost climbs, which makes sense because there is less time to perform maneuvers during the shorter transfers. Beyond 90 days, there are launch periods with low  $\Delta V$  requirements for any transfer duration.

It is expected that the launch period's  $\Delta V$  cost is dependent upon the reference transfer's natural Earth departure inclination. It is hypothesized that a reference transfer that departs the Earth with an inclination near  $28.5^\circ$  will generate a launch period that requires less total  $\Delta V$  than a reference transfer that departs the Earth with an inclination far different. Figure 12 tracks the launch period  $\Delta V$  cost of the 288 missions constructed here as a function of their reference departure inclination values. The right plot in Figure 12 observes the range of transfer  $\Delta V$  values as a function of the difference between the reference departure inclination value and the target  $28.5^\circ$  value. A line has been fit to the maximum  $\Delta V$  for each launch period using a least-squares approach, which yields the relationship:

$$\text{Launch Period } \Delta V \sim (0.470 \text{ m/s/deg}) \times x + 756.5 \text{ m/s},$$

where  $x$  is equal to the absolute value of the difference between the reference departure inclination and  $28.5^\circ$ . The sample set of lunar transfers includes low- $\Delta V$  and high- $\Delta V$  missions, which may swamp any significant relationship between the launch period's  $\Delta V$  cost and the reference departure inclination. Nevertheless, it is very interesting to observe that the launch period's  $\Delta V$  cost does not present a strong correlation with the reference departure inclination.

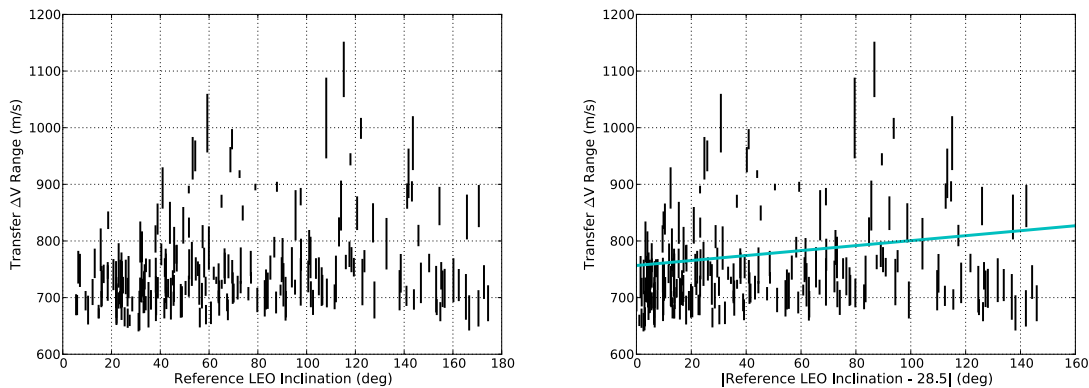


**Figure 12. The range of transfer  $\Delta V$  costs contained in each 21-day launch period as a function of the reference transfer's Earth departure inclination (left) and the absolute value of the difference between the reference inclination and  $28.5^\circ$  (right).**

To further test the relationship of a launch period to the reference LEO inclination, each launch period's  $\Delta V$  has been reduced by its reference  $\Delta V$  so that each launch period may be more closely compared. Figure 13 shows the same two plots as shown in Figure 12, but with each mission's reference  $\Delta V$  subtracted from its launch period  $\Delta V$  range. One can see that the launch period  $\Delta V$  is not well-correlated with the reference departure inclination. The linear fit has a slope of only 0.206 m/s per degree of inclination away from  $28.5^\circ$ . It appears that a 21-day launch period absorbs most of the  $\Delta V$  penalty associated with inclination variations. The natural Earth departure inclination of a transfer certainly varies with transfer duration, and it has already been noticed that the launch period is often not centered about the reference transfer's TLI date. This result is useful,

because it indicates that the natural Earth departure inclination is not a good predictor of the launch period  $\Delta V$  requirement of a reference transfer. The relationship of the low-energy transfer  $\Delta V$  and the TLI inclination will be further explored in the next section.

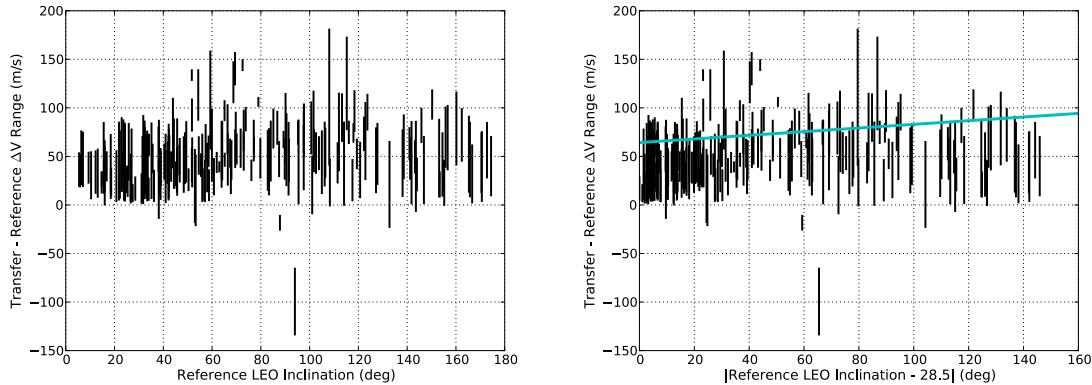


**Figure 13.** The same two plots as shown in Figure 12, but with each mission’s reference  $\Delta V$  subtracted from its 21-day launch period  $\Delta V$  range.

### Varying the LEO Inclination

The results presented previously in this paper have only considered missions that begin in a LEO parking orbit at an inclination of  $28.5^\circ$  relative to the equator, corresponding to launch sites such as Cape Canaveral, Florida. Spacecraft missions certainly depart the Earth from other launch sites; launch vehicles from those sites typically deliver the most mass to low Earth orbit if they launch into a parking orbit at an inclination approximately equal to their launch site’s latitude. Hence, it is of interest to determine the  $\Delta V$  cost required to depart the Earth from any LEO inclination and transfer to the same lunar orbit using a particular low-energy reference transfer.

The algorithms described in this paper have been used to generate missions that depart the Earth from LEO parking orbits at a wide range of inclinations and then target the same reference low-energy transfer discussed earlier (described in Table 2 and illustrated in Figure 3). The reference trajectory naturally departs the Earth on April 1st, 2010 from an orbital inclination of approximately  $38.305^\circ$ ; hence, a mission that departs the Earth at that time from that orbit requires no deterministic maneuvers en route to the Moon. Upon arrival at the Moon, the reference trajectory requires a 649.0 m/s orbit insertion maneuver to impulsively enter the desired 100-km circular lunar orbit. Any mission that departs the Earth from a different inclination will require deterministic TCMs and/or a different orbit insertion maneuver.

Figure 14 illustrates how the deterministic  $\Delta V$  varies for missions that depart the Earth at different LEO inclination values and target the same lunar orbit. The dates and times of the trans-lunar injection and lunar orbit insertion are fixed. The total transfer  $\Delta V$  is shown on the left and the difference between each mission’s total  $\Delta V$  compared to the reference transfer’s total  $\Delta V$  is shown on the right. One can see that the  $\Delta V$  cost of the mission rises as a function of the difference between the mission’s departure inclination and the reference transfer’s departure inclination. The cost is approximately 0.97 m/s per degree of inclination change for missions with LEO inclinations greater than 20 degrees. The transfer cost increases much more rapidly as a mission’s departure approaches equatorial. As the departure inclination drops, the system gradually loses a degree of freedom: the

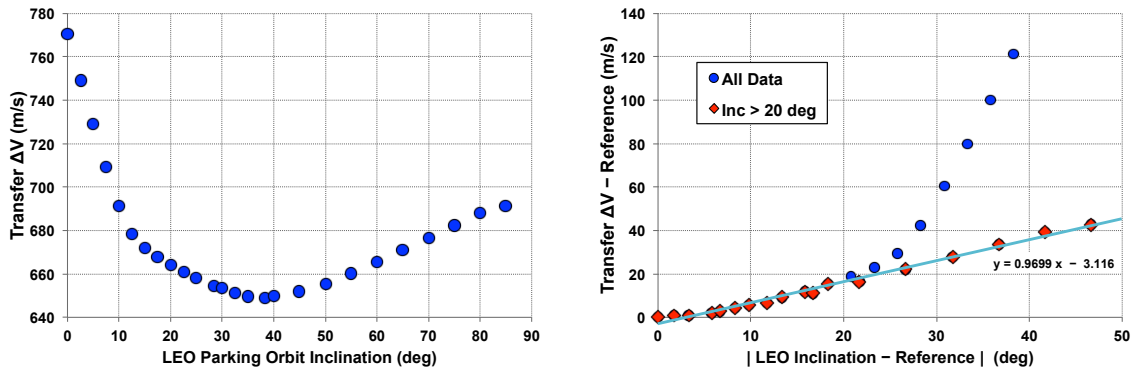


**Figure 14. Left: the total transfer  $\Delta V$  for missions that depart the Earth on April 1, 2010 at different inclinations and arrive at the same reference lunar orbit. Right: the difference in the total transfer  $\Delta V$  for these missions compared with the reference low-energy transfer, which departs at an inclination of  $38.305^\circ$ .**

LEO parking orbit's ascending node becomes less influential on the geometry of the departure. The ascending node is no longer defined for equatorial departures, and the lunar transfer requires over 120 m/s more deterministic  $\Delta V$  than the reference transfer.

As Figure 14 illustrates, the total  $\Delta V$  of a mission to the reference lunar orbit is minimized if the LEO parking orbit has an inclination of  $38.305^\circ$ , provided that the trans-lunar injection is performed on April 1st, 2010. If the TLI date is shifted, then the optimal LEO inclination is likely to shift as well. Hence, the  $\Delta V$  cost of a full 21-day launch period cannot be strictly predicted by observing the difference in inclination between a desired LEO parking orbit and the reference departure.

Figure 15 illustrates three launch periods, corresponding to missions that depart from LEO parking orbits with inclinations of 20, 50, and 80 degrees. One can see that the launch period shifts in time, illustrating that the transfer duration may significantly alter the reference trajectory's natural departure inclination. Figure 16 illustrates the total transfer  $\Delta V$  for each launch opportunity of a 21-day launch period departing from a wide range of departure inclinations. One can see that the launch period  $\Delta V$  is dramatically higher for low inclinations, and the  $\Delta V$  changes very little from one inclination to another for higher inclination values. It is interesting that the missions with higher inclinations require less  $\Delta V$  than missions near the reference transfer's departure inclination. The low- $\Delta V$  points in the lower-left part of the plot correspond to brief opportunities in those launch periods when the Moon passes through an ideal location in its orbit to reduce the transfer  $\Delta V$ .

## CONCLUSIONS

This study has randomly sampled 288 different low-energy transfers between the Earth and polar orbits about the Moon and has constructed practical 21-day launch periods for each of them, using a  $28.5^\circ$  LEO parking orbit and no more than two deterministic maneuvers. The lunar orbits have a wide range of geometries, though they are all polar and have an altitude of approximately 100 km. The reference low-energy transfers include no Earth phasing orbits nor close lunar flybys and require between 65 and 160 days of transfer duration. Each mission has been constructed by using a sequence of steps, varying eight parameters to minimize the transfer  $\Delta V$  cost. The eight variable parameters include the parking orbit's ascending node, the trans-lunar injection's location in the parking orbit, the trans-lunar injection's  $\Delta V$ , the times of two deterministic maneuvers en

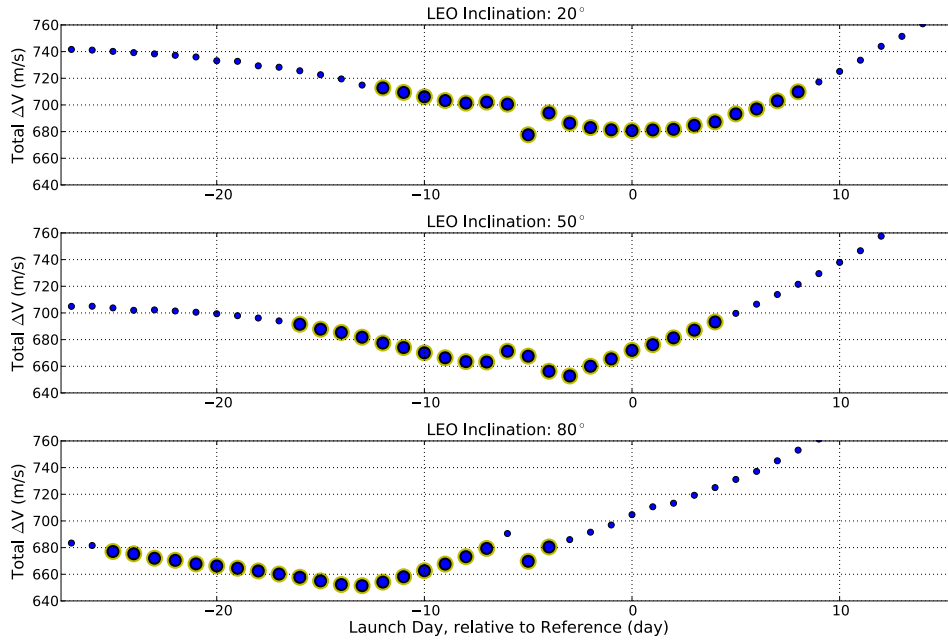


**Figure 15.** Three launch periods for missions to the reference lunar orbit, where each launch period is designed to accommodate a specific LEO inclination; namely,  $20^\circ$  (top),  $50^\circ$  (middle), and  $80^\circ$  (bottom). The Moon perturbs the outbound trajectories for those missions that launch about 5 days before the reference transfer.

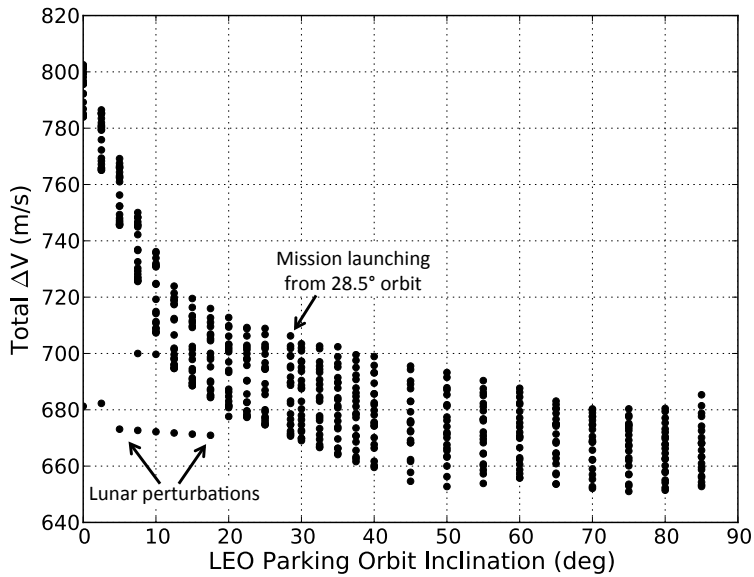


**Figure 16.** The total transfer  $\Delta V$  for each opportunity of a 21-day launch period for missions to the reference lunar orbit departing from LEO parking orbits with varying inclination values.

route to the Moon, and three components of the lunar orbit insertion maneuver. All other aspects of the transfer are fixed when building a particular mission.

Several conclusions may be easily drawn from the results presented in this paper. First of all, the cost of a launch period is obviously dependent on the number of launch days in the period. The transfers constructed here demonstrate that it costs on average approximately 2.5 m/s per day added to a launch period; hence, the average 21-day launch period requires about 50 m/s more deterministic  $\Delta V$  than a 1-day launch period for a given transfer. The cost of establishing a 21-day launch period to the 288 reference transfers studied in this paper is approximately  $71.7 \pm 29.7$  m/s ( $1\sigma$ ), where the additional  $\Delta V$  above and beyond the 50 m/s is required to accommodate a departure from a  $28.5^\circ$  LEO parking orbit. The 21 opportunities in the launch period may be on 21 consecutive days, and frequently are, but typically include one or two gaps. The average launch period for these 288 missions requires a total of 27 days; the vast majority of the launch periods may be contained within 40 days. Finally, it has been found that there is no significant trend between the total launch period  $\Delta V$  for these 288 missions and their reference departure inclination values or their reference transfer durations, except for short transfers with durations below 90 days.

An additional study has been performed to observe how a mission's  $\Delta V$  changes as a function of the particular LEO inclination selected. A mission that departs at a particular time requires approximately 0.97 m/s more transfer  $\Delta V$  per degree of inclination change performed, assuming that the departure inclination is above  $20^\circ$ . The total transfer  $\Delta V$  cost increases dramatically as the departure inclination approaches  $0^\circ$ . These trends change when considering a full 21-day launch period. The required launch period  $\Delta V$  is still high for missions that depart from nearly equatorial LEO parking orbits, but the variation in the launch period  $\Delta V$  is reduced for missions that depart at higher inclinations.

The work presented in this paper is useful for mission designers to gain an understanding about the transfer  $\Delta V$  costs associated with establishing a realistic 21-day launch period from a desirable departure to a particular low-energy lunar transfer.

## Acknowledgements

This work could not have been performed without the support of Ted Sweetser, whose efforts made this work possible. The authors would also like to thank Ted and Roby Wilson for their valuable feedback during the editing of this paper.

The research presented in this paper has been carried out at the Jet Propulsion Laboratory, California Institute of Technology, under a contract with the National Aeronautics and Space Administration. Copyright 2011 California Institute of Technology. Government sponsorship acknowledged.

## REFERENCES

- [1] E. A. Belbruno and J. Miller, "A Ballistic Lunar Capture Trajectory for the Japanese Spacecraft Hiten," Tech. Rep. IOM 312/90.4-1731-EAB, JPL, California Institute of Technology, 1990.
- [2] K. Uesugi, "Japanese first double Lunar swingby mission 'HITEN'," *Acta Astronautica*, Vol. 25, No. 7, 1991, pp. 347–355.
- [3] S. B. Broschart, M. J. Chung, S. J. Hatch, J. H. Ma, T. H. Sweetser, S. S. Weinstein-Weiss, and V. Angelopoulos, "Preliminary Trajectory Design for the ARTEMIS Lunar Mission," *AAS/AIAA Astrodynamics Specialist Conference*, No. AAS 09-382, Pittsburgh, Pennsylvania, AAS/AIAA, August 9–13, 2009.
- [4] M. Woodard, D. Folta, and D. Woodfork, "ARTEMIS: The First Mission to the Lunar Libration Orbits," *21st International Symposium on Space Flight Dynamics*, Toulouse, France, Centre National d'Études Spatiales, September 28 – October 2, 2009.

- [5] R. B. Roncoli and K. K. Fujii, "Mission Design Overview for the Gravity Recovery and Interior Laboratory (GRAIL) Mission," *AIAA/AAS Astrodynamics Specialist Conference*, No. AIAA 2010-8383, Toronto, Ontario, Canada, AIAA/AAS, August 2–5, 2010.
- [6] M. J. Chung, S. J. Hatch, J. A. Kangas, S. M. Long, R. B. Roncoli, and T. H. Sweetser, "Trans-Lunar Cruise Trajectory Design of GRAIL (Gravity Recovery and Interior Laboratory) Mission," *AIAA/AAS Astrodynamics Specialist Conference*, No. AIAA 2010-8384, Toronto, Ontario, Canada, AIAA/AAS, August 2–5, 2010.
- [7] S. J. Hatch, R. B. Roncoli, and T. H. Sweetser, "GRAIL Trajectory Design: Lunar Orbit Insertion through Science," *AIAA/AAS Astrodynamics Specialist Conference*, No. AIAA 2010-8385, Toronto, Ontario, Canada, AIAA/AAS, August 2–5, 2010.
- [8] J. S. Parker, R. L. Anderson, and A. Peterson, "A Survey of Ballistic Transfers to Low Lunar Orbit," *AAS/AIAA Space Flight Mechanics Meeting*, No. AAS 11-277, New Orleans, LA, AAS/AIAA, Feb 13–17, 2011.
- [9] J. S. Parker, *Low-Energy Ballistic Lunar Transfers*. PhD thesis, University of Colorado, Boulder, Colorado, 2007.
- [10] J. S. Parker and G. H. Born, "Modeling a Low-Energy Ballistic Lunar Transfer Using Dynamical Systems Theory," *Journal of Spacecraft and Rockets*, Vol. 45, Nov–Dec 2008, pp. 1269–1281.
- [11] J. S. Parker, "Low-Energy Ballistic Transfers to Lunar Halo Orbits," *AAS/AIAA Astrodynamics Specialist Conference*, No. AAS 09-443, Pittsburgh, Pennsylvania, AAS/AIAA, August 9–13, 2009.
- [12] J. S. Parker, "Targeting Low-Energy Ballistic Lunar Transfers," *American Astronautical Society, George H. Born Special Symposium*, Boulder, Colorado, AAS, May 13–14, 2010.
- [13] C. Conley, "Low Energy Transit Orbits in the Restricted Three Body Problem," *SIAM Journal Appl. Math.*, Vol. 16, No. 4, 1968, pp. 732–746.
- [14] V. V. Ivashkin, "On Trajectories of the Earth-Moon Flight of a Particle with its Temporary Capture by the Moon," *Doklady Physics, Mechanics*, Vol. 47, No. 11, 2002, pp. 825–827.
- [15] V. V. Ivashkin, "On Particle's Trajectories of Moon-to-Earth Space Flights with the Gravitational Escape from the Lunar Attraction," *Doklady Physics, Mechanics*, Vol. 49, No. 9, 2004, pp. 539–542.
- [16] W. S. Koon, M. W. Lo, J. E. Marsden, and S. D. Ross, "Shoot the Moon," *AAS/AIAA Spaceflight Mechanics 2000*, Vol. 105, part 2, AAS/AIAA, 2000, pp. 1017–1030.
- [17] R. L. Anderson and J. S. Parker, "A Survey of Ballistic Transfers to the Lunar Surface," *AAS/AIAA Space Flight Mechanics Meeting*, No. AAS 11-278, New Orleans, LA, AAS/AIAA, Feb 13–17, 2011.
- [18] E. M. Alessi, G. Gómez, and J. J. Masdemont, "Leaving the Moon by Means of Invariant Manifolds of Libration Point Orbits," *Communications in Nonlinear Science and Numerical Simulation*, Vol. 14, December 2009, pp. 4153–4167.
- [19] L. Lozier, K. Galal, D. Folta, and M. Beckman, "Lunar Prospector Mission Design and Trajectory Support," *AAS/AIAA Spaceflight Dynamics Conference*, No. AAS 98-323, AAS/AIAA, 1998.
- [20] A. Matsuoka and C. T. Russell, eds., *The Kaguya Mission to the Moon*. New York, NY: Springer, first ed., 2011.
- [21] NASA, "NASA National Space Science Data Center (NSSDC) Lunar and Planetary Home Page," August 2006.
- [22] J. N. Goswami and M. Annadurai, "Chandrayaan-1: India's First Planetary Science Mission to the Moon," *Current Science; Special Section: Chandrayaan-1*, Vol. 96, 25 February 2009, pp. 486–491.
- [23] M. Beckman, "Mission Design for the Lunar Reconnaissance Orbiter," *29th Annual AAS Guidance and Control Conference*, No. AAS 07-057, Breckenridge, CO, AAS, 2007.
- [24] V. Szebehely, *Theory of Orbits: The Restricted Problem of Three Bodies*. New York: Academic Press, 1967.
- [25] R. B. Roncoli, "Lunar Constants and Models Document," Tech. Rep. JPL D-32296, Jet Propulsion Laboratory, California Institute of Technology, September 2005.
- [26] F. T. Krogh, "Variable Order Adams Method for Ordinary Differential Equations," tech. rep., California Institute of Technology, 2010 Math à la Carte, Inc., <http://mathalacarte.com/cb/mom.fcg/ya64>, Tujunga, California, October 1975.
- [27] W. M. Folkner, J. G. Williams, and D. H. Boggs, "The Planetary and Lunar Ephemeris DE 421," Tech. Rep. IOM 343R–08–003, Jet Propulsion Laboratory, California Institute of Technology, March 2008. [ftp://naif.jpl.nasa.gov/pub/naif/generic\\_kernels/spk/planets/de421\\_announcement.pdf](ftp://naif.jpl.nasa.gov/pub/naif/generic_kernels/spk/planets/de421_announcement.pdf).
- [28] P. E. Gill, W. Murray, and M. A. Saunders, "User's Guide for SNOPT 7.1: A Fortran Package for Large-Scale Nonlinear Programming," Tech. Rep. Numerical Analysis Report NA 04-1, Department of Mathematics, University of California, San Diego, La Jolla, CA, 2004.
- [29] P. E. Gill, W. Murray, and M. A. Saunders, "SNOPT: An SQP Algorithm for Large-Scale Constrained Optimization," *SIAM Review*, Vol. 47, No. 1, 2005, pp. 99–131.
- [30] R. S. Wilson and K. C. Howell, "Trajectory Design in the Sun-Earth-Moon System Using Lunar Gravity Assists," *Journal of Spacecraft and Rockets*, Vol. 35, No. 2, 1998, pp. 191–198.